

# Acceleration of electrons from rest to GeV energies by ultrashort transverse magnetic laser pulses in free space

Charles Varin\* and Michel Piché

*Centre d'Optique, Photonique et Laser, Université Laval, Sainte-Foy, Québec, Canada G1K 7P4*

Miguel A. Porras

*Departamento de Física Aplicada, Escuela Técnica Superior de Ingenieros de Minas, Universidad Politécnica de Madrid, Ríos Rosas 21, E-28003 Madrid, Spain*

(Received 25 April 2004; published 8 February 2005)

In this paper we describe a laser acceleration scheme where an electron is accelerated from rest to GeV energies by the longitudinal electric field of an ultrashort transverse magnetic (TM<sub>01</sub>) optical pulse. The on-axis longitudinal electric field of the pulse is obtained from the free-space divergence equation beyond the so-called slowly-varying-envelope approximation. The instantaneous electron dynamics is studied; numerical simulations predict net energy gains in the GeV range for laser intensities reaching 10<sup>22</sup> W/cm<sup>2</sup>.

DOI: 10.1103/PhysRevE.71.026603

PACS number(s): 41.20.-q, 03.50.De, 96.50.Pw, 41.75.Jv

## I. INTRODUCTION

Laser-driven accelerators are considered as a potential scheme to build experimental facilities that produce high-energy particle beams, with reduced size and lower cost compared to accelerators presently in use [1–4]. To operate laser-driven accelerators in a traveling-wave configuration, the displacement of charged particles must be synchronized with the phase of the driving electromagnetic field. Once synchronization is achieved, the moving charges feel a static electric field and they are accelerated for a finite period of time. Metal waveguides [5,6], plasmas [7,8], inverse free-electron lasers [9], self-sustained cyclotron resonance [10], vacuum beat waves [11], focused doughnut pulses [12], sub-cycle pulses [13,14], laser beams with sharp-rising edges [15,16], evanescent waves [17], and photonic band gap fibers [18] are some of the acceleration schemes that have been proposed within the past 40 years. As it is discussed in Refs. [19–25], acceleration schemes that involve laser beams in free space offer some practical advantages.

In this paper, we describe an approach to laser acceleration in free space based on the longitudinal electric field associated with a transverse magnetic (TM<sub>01</sub>) beam with a very short duration in the time domain. We have selected the TM<sub>01</sub> beam because in the paraxial approximation it experiences a phase advance of  $\pi$ —known as the Gouy phase shift—from its waist to infinity. Hence, it should be possible to confine a relativistic charged particle within a half cycle of the on-axis longitudinal electric field. In principle, this partial synchronization should produce a substantial acceleration. To carry out the analysis of this proposed scheme, the vectorial propagation of an ultrashort TM<sub>01</sub> wave packet is considered and the longitudinal electric field is calculated from the free-space divergence equation beyond the slowly-varying-envelope approximation (SVEA). Through numerical simulations, we investigate the on-axis dynamics of elec-

trons initially at rest at the focal plane of an ultrashort TM<sub>01</sub> wave packet. From real-time integration of the instantaneous Lorentz force, we demonstrate that some electrons can be captured by the field. When the laser intensity reaches 10<sup>22</sup> W/cm<sup>2</sup>, captured electrons are accelerated to GeV energies within a few millimeters.

The paper is divided as follows. In Sec. II we establish the full electromagnetic structure of ultrafast TM<sub>01</sub> wave packets propagating in free space. We therein develop a procedure to correct the SVEA when the electromagnetic field lasts only a few optical cycles. Section III deals with the dynamics of on-axis electrons subject to the acceleration caused by the longitudinal electric field component of the TM<sub>01</sub> wave packet. We also consider the stability of the on-axis electron trajectory with respect to the radial field components, as well as the losses caused by the emission of radiation during acceleration. In Sec. IV our method is compared to other proposed schemes, including those based on the focusing of doughnut-shape modes and on the ponderomotive potential. We also discuss the presence of any effect caused by residual static field components.

## II. VECTORIAL DESCRIPTION OF ULTRASHORT TM<sub>01</sub> LASER WAVE PACKETS FOCUSED IN FREE SPACE

A focused TM<sub>01</sub> beam is characterized by a ring-shaped (doughnut-shaped) intensity profile. It can be generated interferometrically from two identical cross-polarized TM<sub>01</sub> Gauss-Hermite modes [26–30]. In this section, we solve Maxwell's divergence equation in free space to obtain the longitudinal electric field of an ultrashort TM<sub>01</sub> wave packet.

### A. The divergence equation beyond the slowly-varying-envelope approximation

The propagation of a laser wave packet is generally studied with the use of a spatiotemporal envelope sustained by a plane-wave carrier. As demonstrated by Brabec and Krausz,

\*Electronic address: charles.varin@phy.ulaval.ca

this approach still applies for tightly focused few-cycle pulses [31,32]. Beyond the so-called slowly-varying-envelope approximation, solutions of Maxwell's equations can be obtained using the method introduced by Lax *et al.* [33]. In this section, we develop a general method—based on the divergence equation of the electric field *in vacuo*—to calculate the longitudinal electric field associated with pulses of a few-cycle duration.

The six field components of an electromagnetic field form a unique vectorial solution of the four Maxwell's equations. Thus, given the transverse electric field  $\mathbf{E}_\perp$ , the longitudinal electric field  $E_z$  can be obtained from the divergence equation

$$\nabla \cdot \mathbf{E} = 0. \quad (1)$$

Using phasor notation, with  $\mathbf{a}_z$  being a longitudinal unit vector oriented along the pulse propagation, we define the vectorial electric field as follows:

$$\begin{aligned} \mathbf{E} &= \mathbf{E}_\perp + E_z \mathbf{a}_z, \\ &= \text{Re}\{\tilde{\mathbf{E}} \exp[j(\omega_0 t - k_0 z)]\} \\ &= \text{Re}\{(\tilde{\mathbf{E}}_\perp + \tilde{E}_z \mathbf{a}_z) \exp[j(\omega_0 t - k_0 z)]\}, \end{aligned} \quad (2)$$

where  $\omega_0 = k_0 c$ ,  $k_0 = 2\pi/\lambda_0$ , and  $\lambda_0$  are, respectively, the central angular frequency, central wave number, and central wavelength of the pulse spectrum, with  $c$  being the speed of light in free space. The complex amplitudes  $\tilde{\mathbf{E}}_\perp$  and  $\tilde{E}_z$  are phasors that are explicitly dependent upon the variables  $x$ ,  $y$ ,  $z$ , and  $t$ . By introducing Eq. (2) in Eq. (1), the divergence equation reads

$$\nabla_\perp \cdot \tilde{\mathbf{E}}_\perp = jk_0 \tilde{E}_z - \frac{\partial \tilde{E}_z}{\partial z}, \quad (3)$$

given  $\nabla_\perp$  to be a two-dimensional differential operator, acting in the plane perpendicular to the  $z$ -oriented time-averaged Poynting vector. Equation (3), which is equivalent to Eq. 4(b) of Ref. [34], can be formally inverted to yield

$$\tilde{E}_z = \sum_{m=0}^{\infty} \left( \frac{-j}{k_0} \right)^{m+1} \frac{\partial^m}{\partial z^m} (\nabla_\perp \cdot \tilde{\mathbf{E}}_\perp). \quad (4)$$

It should be noticed that no approximation is necessary to obtain Eq. (4) from Eq. (3). Hence, it applies to both non-paraxial beams and few-cycle pulses: if the spatial distribution and polarization of the transverse electric field  $\mathbf{E}_\perp$  are known, it gives an exact expression of the corresponding longitudinal electric field  $E_z$ . The  $m=0$  term is the contribution to the longitudinal electric field that originates from the carrier of the transverse electric field and all higher-order terms—the  $m=1, 2, 3, \dots, \infty$  terms—are contributions coming from the transverse field envelope  $\tilde{\mathbf{E}}_\perp$ . For slightly focused and long pulses, Eq. (4) reduces to the expression for paraxial and monochromatic beams [28,33].

### B. The longitudinal electric field of an ultrashort $\text{TM}_{01}$ laser wave packet in free space

As has been mentioned before, a  $\text{TM}_{01}$  wave packet can be generated by an interferometric method [26]. As a conse-

quence of the interference between the overlapping beams, the signal intensity is zero on the axis [27]. For a propagation oriented along the  $z$  axis of the cylindrical coordinate system  $(r, \theta, z)$ , its transverse electric field  $\mathbf{E}_\perp$  is radially polarized and angularly symmetric, i.e.,  $\mathbf{E}_\perp = E_r \mathbf{a}_r$  and  $\partial_\theta \mathbf{E}_\perp = 0$ .

Following the work of Porras [35], we express the electric field of a scalar ultrashort pulsed beam beyond the SVEA as a series of corrections to a paraxial quasimonochromatic beam. For the  $\text{TM}_{01}$  laser beam, the zeroth-order transverse field is defined as

$$\tilde{E}_r^{(0)} = A \left( \frac{jz_R}{\tilde{q}} \right)^2 r \exp\left(-j \frac{k_0 r^2}{2\tilde{q}}\right) f(t') \quad (5a)$$

$$= -A \frac{z_R}{k_0} \frac{\partial G_0}{\partial r} f(t'), \quad (5b)$$

where  $A$  is a normalizing constant,  $\tilde{q} = z' + jz_R$  is the complex parameter of the Gaussian beam,  $G_0 = (jz_R/\tilde{q}) \times \exp(-jk_0 r^2/2\tilde{q})$  is the fundamental Gaussian-beam spatial envelope,  $f(t') = \exp(-t'^2/T^2)$  is a Gaussian pulse envelope with  $T$  being the pulse duration, and  $z_R = k_0 \rho_0^2/2$  is the Rayleigh distance with  $\rho_0$  being the beam spot size at the beam waist [27]. The retarded time  $t'$  is introduced as a new variable to distinguish diffraction (which depends on  $z' = z$ ) from temporal effects (which depend on  $t' = t - z/c$ ). By recalling the method outlined in Ref. [35] [see Eqs. (8)–(11)], the  $n$ th-order correction then reads

$$\tilde{E}_r^{(n)} = \left( \frac{j}{\omega_0} \right)^n \frac{\partial^n}{\partial t'^n} \frac{\partial^{n-1}}{\partial z'^{n-1}} \left( \frac{z'^n}{n!} \frac{\partial \tilde{E}_r^{(0)}}{\partial z'} \right) \quad (6a)$$

$$= -A \frac{z_R}{k_0} \left( \frac{j}{\omega_0} \right)^n \frac{\partial^n f(t')}{\partial t'^n} \frac{\partial G_0^{(n)}}{\partial r}, \quad (6b)$$

where  $n=1, 2, 3, \dots$  and

$$G_0^{(n)} = G_0 \sum_{p=1}^n \binom{n-1}{p-1} \left( \frac{-z'}{\tilde{q}} \right)^p L_p \left( j \frac{k_0 r^2}{2\tilde{q}} \right), \quad (7)$$

with  $\binom{n-1}{p-1}$  being the binomial coefficient and  $L_p(\cdot)$  the Laguerre polynomial of order  $p$ . By definition,  $G_0^{(0)} = G_0$ . As defined in Eq. (2), the physical field is the real part of the complex envelope times the carrier wave. Thus,

$$\mathbf{E}_\perp = \text{Re} \left[ \left( \tilde{E}_r^{(0)} + \sum_{n=1}^{\infty} \tilde{E}_r^{(n)} \right) \mathbf{a}_r \exp[j(\omega_0 t' - \phi_0)] \right], \quad (8)$$

where  $\phi_0$  is the carrier phase at the beam waist.

For a paraxial few-cycle wave packet, we have [35]

$$\partial_z \tilde{\mathbf{E}}_{\perp} = \partial_z \tilde{\mathbf{E}}_{\perp} - c^{-1} \partial_t \tilde{\mathbf{E}}_{\perp} \quad (9a)$$

$$\simeq -c^{-1} \partial_t \tilde{\mathbf{E}}_{\perp} \quad (9b)$$

$$\simeq -c^{-1} \partial_t \left( \tilde{\mathbf{E}}_r^{(0)} + \sum_{n=1}^{\infty} \tilde{\mathbf{E}}_r^{(n)} \right) \mathbf{a}_r. \quad (9c)$$

By introducing Eq. (9b) in Eq. (4), it is easily shown that for each correction applied to the transverse field there corresponds a contribution to the longitudinal field given by the following expression:

$$\tilde{E}_z^{(n')} = -\frac{j}{k_0} \sum_{m=0}^{\infty} \left( \frac{j}{\omega_0} \right)^m \frac{\partial^m}{\partial t'^m} (\nabla_{\perp} \cdot \tilde{\mathbf{E}}_{\perp}^{(n')}), \quad (10)$$

where  $n'=(n-1)=0,1,2,3,\dots$ . After calculation with Eqs. (5), (6), and (10), the zeroth-order ( $n'=0$  and  $m=0,1,2,3,\dots$ ) longitudinal electric field reads

$$\tilde{E}_z^{(0)} = -2j \frac{A}{k_0} \left( \frac{jz_R}{\tilde{q}} \right)^2 \left[ 1 - j \frac{k_0 r^2}{2\tilde{q}} \right] \exp\left(-j \frac{k_0 r^2}{2\tilde{q}}\right) f_z^{(0)}(t'), \quad (11)$$

and the  $n$ th longitudinal correction ( $n=1,2,3,\dots$  and  $m=0,1,2,3,\dots$ ) is written as

$$\tilde{E}_z^{(n)} = A \frac{jz_R}{k_0^2} f_z^{(n)}(t') \frac{1}{r} \frac{\partial}{\partial r} \left[ r \frac{\partial G_0^{(n)}}{\partial r} \right], \quad (12)$$

where  $f_z^{(n)}(t')$  is the time envelope of the longitudinal field:

$$f_z^{(n)}(t') = \sum_{m=0}^{\infty} \left( \frac{j}{\omega_0} \right)^{m+n'} \partial_t'^{m+n'} f(t') \quad (13a)$$

$$= \exp\left(-\frac{t'^2}{T^2}\right) \sum_{m=0}^{\infty} \left( \frac{-j}{\omega_0 T} \right)^{m+n'} H_{m+n'}\left(\frac{t'}{T}\right), \quad (13b)$$

with  $H_{m+n'}(x)$  being the Hermite polynomial of order  $(m+n')$ .

As shown in Fig. 1, the transverse electric field vanishes on axis ( $r=0$ ), as the longitudinal electric field reaches its maximal value. Since  $(E_z)_{max} \propto \lambda_0 / \rho_0 (E_r)_{max}$ , the amplitude of the longitudinal electric field is only a small fraction of the amplitude of the transverse electric field. From Eqs. (11) and (12), the zeroth-order and  $n$ th-order contributions to the on-axis longitudinal field  $\tilde{E}_z$  are found to be

$$\tilde{E}_z^{(0)} = -2j \frac{A}{k_0} \left( \frac{jz_R}{\tilde{q}} \right)^2 f_z^{(0)}, \quad (14)$$

$$\tilde{E}_z^{(n)} = -2j \frac{A}{k_0} \left( \frac{jz_R}{\tilde{q}} \right)^2 f_z^{(n)} \sum_{p=1}^n \binom{n-1}{p-1} (p+1) \left( \frac{-z'}{\tilde{q}} \right)^p. \quad (15)$$

The physical on-axis longitudinal electric field  $\mathbb{E}_z$  is defined as

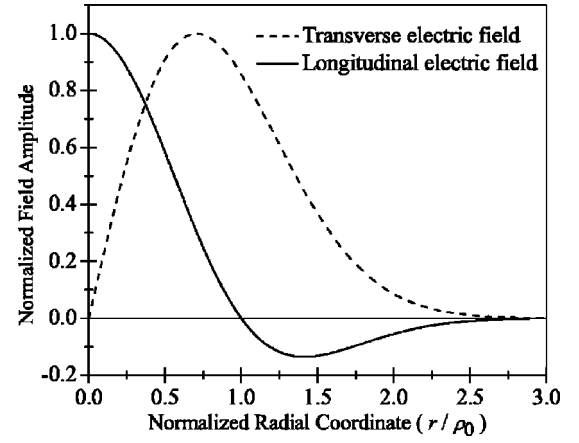


FIG. 1. Spatial distribution of the transverse (dashed line) and longitudinal (full line) electric fields of a  $TM_{01}$  wave packet at the waist ( $z'=0$ ). Fields are not to scale: they have been normalized so that their respective maxima are equal to 1.

$$\mathbb{E}_z = \text{Re} \left[ \left( \tilde{E}_z^{(0)} + \sum_{n=1}^{\infty} \tilde{E}_z^{(n)} \right) \exp[j(\omega_0 t' - \phi_0)] \right]. \quad (16)$$

When the pulse duration is long compared to the carrier oscillations, i.e., when  $T \gg 2\pi/\omega_0$ , the SVEA applies and  $\tilde{E}_z \simeq \tilde{E}_z^{(0)}$ . On the other hand, as the pulse duration decreases and approaches the limit of a single-cycle pulse ( $T = 2\pi/\omega_0$ ), higher-order terms become significant and modify noticeably the pulse envelope and carrier oscillations (see Fig. 2). As a result, the carrier wave is redshifted (slower oscillations) between the beam waist ( $z'=0$ ) and the Rayleigh distance ( $z'=z_R$ ) and blueshifted (faster oscillations) beyond this position. Also, the pulse envelope appears to be slowed down (positive time delay) between  $z'=0$  and  $\infty$ , but faster (negative time delay) between  $z'=-\infty$  and 0. In Fig. 3, these two effects are compared to the SVEA field for  $z' \geq 0$ .

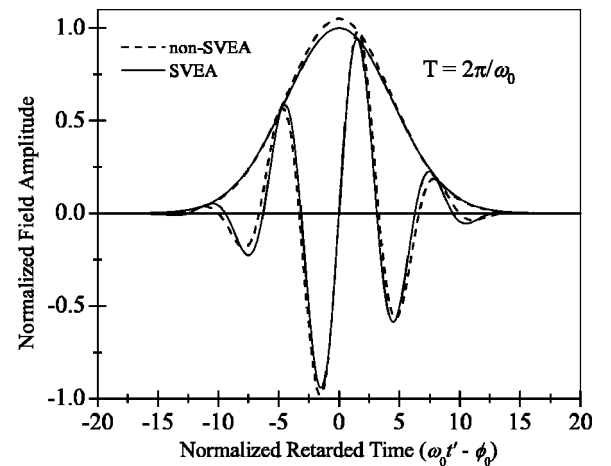


FIG. 2. Envelope and oscillations of the on-axis longitudinal electric field  $\mathbb{E}_z$  of a single-cycle ( $T=2\pi/\omega_0$ )  $TM_{01}$  wave packet with a Gaussian temporal envelope at the waist ( $z'=0$ ). The SVEA field corresponds to  $n'=0$ ,  $m=0$  and the non-SVEA field to  $n'=0,1,2$ ,  $m=0,1,2$ .

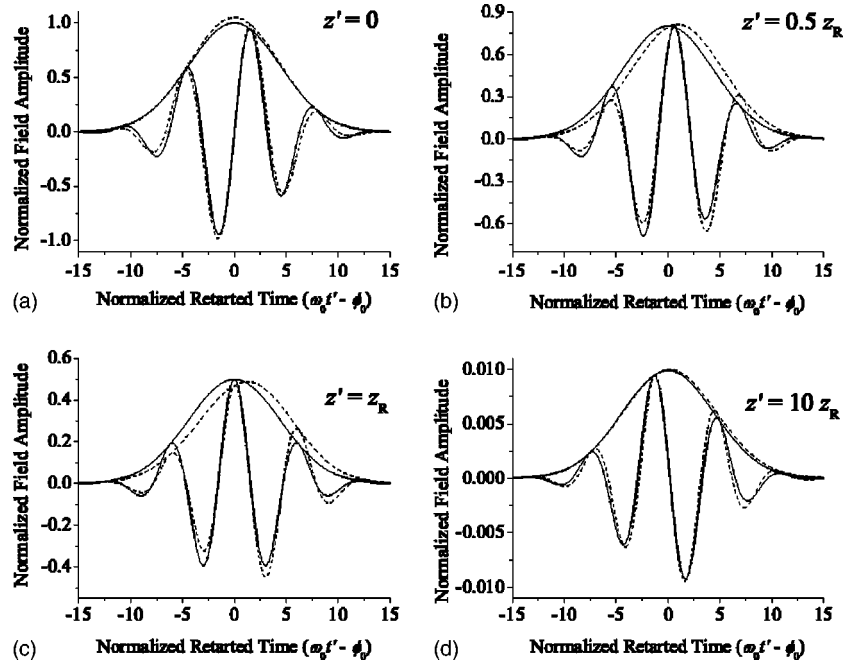


FIG. 3. On-axis envelope and oscillations of the longitudinal electric field of a single-cycle ( $T=2\pi/\omega_0$ )  $\text{TM}_{01}$  wave packet. The non-SVEA field (dashed curve), i.e., the corrected field with the terms corresponding to  $n'=0,1,2$  and  $m=0,1,2$ , is compared to the quasimonochromatic (SVEA) field (solid curve) for different axial positions  $z'$ .

Finally, the wave carrier experiences a global on-axis (Gouy) phase shift of  $\pi$  from  $z'=0$  to  $\infty$ , thus offering the possibility of synchronizing charged particles with the field within this range.

### C. The magnetic flux vector of an ultrashort $\text{TM}_{01}$ laser wave packet in free space

A general equation giving the magnetic flux vector  $\mathbf{B}$  of an arbitrary ultrashort wave packet cannot always be reduced to a simple expression, as is the case for monochromatic transverse electromagnetic (TEM) waves [see Eq. (7.11) of Ref. [36]]. However, when the electric field vector is known,  $\mathbf{B}$  can easily be deduced through Maxwell's equations.

For the  $\text{TM}_{01}$  wave packet,  $B_z=0$ ,  $E_\theta=0$ , and  $B_r=0$ . Furthermore, if the divergence equation for the electric field is satisfied, the differential form of Ampère's law in free space, i.e.,  $\nabla \times \mathbf{B} = c^{-2} \partial_t \mathbf{E}$ , leads to the following equation:

$$-\frac{\partial B_\theta}{\partial z} = \frac{1}{c^2} \frac{\partial E_r}{\partial t}. \quad (17)$$

Introducing phasor notation, Eq. (17) becomes

$$\tilde{B}_\theta + \frac{j}{k_0} \frac{\partial \tilde{B}_\theta}{\partial z} = \frac{1}{c} \left( \tilde{E}_r - \frac{j}{\omega_0} \frac{\partial \tilde{E}_r}{\partial t} \right). \quad (18)$$

The technique introduced in Sec. II A, previously used by Haselhoff to develop a high-gain free-electron-laser model [34], can be applied to obtain  $B_\theta$ . However, under the paraxial approximation [see Eq. (9b)], Eq. (18) exactly yields

$$\tilde{B}_\theta = \frac{1}{c} \tilde{E}_r. \quad (19)$$

## III. DYNAMICS OF AN ELECTRON IN AN ULTRASHORT $\text{TM}_{01}$ LASER WAVE PACKET FOCUSED IN FREE SPACE

In this section, we explain the steps followed to study the motion of an electron initially at rest at the beam waist of an intense ultrashort  $\text{TM}_{01}$  laser wave packet. The analysis presented here, based on the instantaneous relativistic Lorentz force, reveals a highly nonlinear dynamics that is not accessible from time-averaged equations [37,38].

### A. Equations of motion

The equations of motion for an electron in an external electromagnetic field are expressed in a relativistic form as [36]

$$\frac{d\mathbf{p}}{dt} = q[\mathbf{E} + \mathbf{v} \times \mathbf{B}], \quad (20)$$

$$\frac{dW}{dt} = q\mathbf{v} \cdot \mathbf{E}, \quad (21)$$

where  $\mathbf{p} = \gamma m_0 \mathbf{v}$  and  $W = \gamma m_0 c^2$  are, respectively, the momentum and energy of an electron of velocity  $\mathbf{v}$ , charge  $q$ , and rest mass  $m_0$ , with  $\gamma = (1 - \mathbf{v}^2/c^2)^{-1/2}$ . Inside the symmetric field of a  $\text{TM}_{01}$  wave packet, Eq. (20) is developed as follows [with the use of Eq. (19)]:

$$\frac{dp_r}{dt} = q \left[ 1 - \frac{v_z}{c} \right] E_r, \quad (22)$$

$$\frac{dp_\theta}{dt} = 0, \quad (23)$$

$$\frac{dp_z}{dt} = q \left[ E_z + \frac{v_r}{c} E_r \right]. \quad (24)$$

Along the axis ( $r=0$ ), the transverse electric field vanishes, leaving only the longitudinal electric field acting on the electron. This field configuration produces an acceleration parallel to the time-averaged Poynting vector [36]. For that ideal case a one-dimensional dynamics is obtained, thus leading, with the help of Eq. (21), to the following equations of motion:

$$\frac{dz}{dt} = v_z, \quad (25)$$

$$\frac{dv_z}{dt} = \frac{q}{m_0} \mathbb{E}_z(z, t) \left[ 1 - \frac{v_z^2}{c^2} \right]^{3/2}, \quad (26)$$

where

$$\mathbb{E}_z(z, t) = \text{Re}\{\tilde{\mathbb{E}}_z \exp[j(\omega_0 t - k_0 z - \phi_0)]\} \quad (27)$$

is the physical on-axis longitudinal electric field obtained from Eqs. (14)–(16). By considering the corrected field shown in Fig. 3, Eq. (27) then reads

$$\begin{aligned} \mathbb{E}_z(z, t) = & 2 \frac{A}{k_0} \left( \frac{\rho_0}{\rho(z)} \right)^2 f(t') \left[ \sin \Psi_0 - \left( \frac{1}{\omega_0 T} \right) H_1 \left( \frac{t'}{T} \right) \cos \Psi_0 - \left( \frac{1}{\omega_0 T} \right)^2 H_2 \left( \frac{t'}{T} \right) \sin \Psi_0 \right] + 4 \frac{A}{k_0} \left( \frac{z}{z_R} \right) \left( \frac{\rho_0}{\rho(z)} \right)^3 f(t') \\ & \times \left[ \left( \frac{1}{\omega_0 T} \right) H_1 \left( \frac{t'}{T} \right) \sin \Psi_1 - \left( \frac{1}{\omega_0 T} \right)^2 H_2 \left( \frac{t'}{T} \right) \cos \Psi_1 - \left( \frac{1}{\omega_0 T} \right)^3 H_3 \left( \frac{t'}{T} \right) \sin \Psi_1 \right] - 4 \frac{A}{k_0} \left( \frac{z}{z_R} \right) \left( \frac{\rho_0}{\rho(z)} \right)^3 f(t') \\ & \times \left[ \left( \frac{1}{\omega_0 T} \right)^2 H_2 \left( \frac{t'}{T} \right) \cos \Psi_1 + \left( \frac{1}{\omega_0 T} \right)^3 H_3 \left( \frac{t'}{T} \right) \sin \Psi_1 - \left( \frac{1}{\omega_0 T} \right)^4 H_4 \left( \frac{t'}{T} \right) \cos \Psi_1 \right] + 6 \frac{A}{k_0} \left( \frac{z}{z_R} \right)^2 \left( \frac{\rho_0}{\rho(z)} \right)^4 f(t') \\ & \times \left[ \left( \frac{1}{\omega_0 T} \right)^2 H_2 \left( \frac{t'}{T} \right) \sin \Psi_2 - \left( \frac{1}{\omega_0 T} \right)^3 H_3 \left( \frac{t'}{T} \right) \cos \Psi_2 - \left( \frac{1}{\omega_0 T} \right)^4 H_4 \left( \frac{t'}{T} \right) \sin \Psi_2 \right], \quad (28) \end{aligned}$$

where  $\Psi_{n'} = \omega_0 t - k_0 z + (2+n')\Psi_G - \phi_0$ ,  $\Psi_G = \tan^{-1}(z/z_R)$  is the basic Gouy phase shift of a paraxial Gaussian beam, and  $\rho(z) = \rho_0 \sqrt{1+z^2/z_R^2}$  is the wave packet transverse dimension. We point out that, according to Eq. (28), the longitudinal electric field of a paraxial and monochromatic  $\text{TM}_{01}$  beam experiences a Gouy phase shift given by  $2\Psi_G$ , and hence a phase advance of  $\pi$  from  $z=0$  to  $\infty$  (for an ultrashort wave packet the actual Gouy phase shift would be slightly larger, as shown recently by Lindner *et al.* [39]). This feature offers the possibility for relativistic electrons to remain in phase with the longitudinal electric field of a  $\text{TM}_{01}$  beam from its waist to infinity. However, an electron initially at rest at the beam waist will not be trapped within a half cycle of the pulse up to  $z=\infty$ ; a delay is necessary to bring the electron from rest to a relativistic velocity. As a consequence of that delay, the electron will slip into the next half cycle where it will be decelerated. During successive acceleration and deceleration cycles, the electron will move away from the beam waist, toward the Rayleigh distance  $z_R$ . From that position to infinity, the Gouy phase shift of a paraxial and monochromatic  $\text{TM}_{01}$  beam is only  $\pi/2$ . If the electron reaches a position around  $z_R$  and if the field intensity is high enough, the electron could then be accelerated to a relativistic velocity and confined within a half cycle of the pulse, up to  $z=\infty$ . In the next subsection, we investigate the dynamics of such electrons using the theoretical tools we developed.

## B. Electron dynamics

The instantaneous electron dynamics is obtained by numerically solving Eqs. (25) and (26). The acceleration of an electron subject to the field of a paraxial ( $\lambda_0=0.8 \mu\text{m}$ ,  $\rho_0=10 \mu\text{m}$ , and  $k_0\rho_0 \approx 78.5$ ) ultrashort ( $T \geq 2\pi/\omega_0$ )  $\text{TM}_{01}$  wave packet that comes from  $z=-\infty$  is considered [40,41]. The electron of rest mass  $m_0=9.109 \times 10^{-31}$  kg and charge  $q=-1.602 \times 10^{-19}$  C is initially at rest ( $v_0=0$ ) at the beam waist ( $z_0=0$ ), where  $v_0$  and  $z_0$  are the initial velocity and position of the electron. The field intensity is defined, in  $\text{W}/\text{cm}^2$ , as  $I=E_0^2/2\eta_0=\rho_0^2 A^2 \exp(-1)/4\eta_0$ , where  $E_0$  is the maximum value of the transverse field amplitude in  $\text{V}/\text{cm}$  and  $\eta_0=120\pi \Omega$  is the impedance of free space.

Through numerical simulations of the instantaneous equations of motion, using an embedded fifth-order Cash-Karp Runge-Kutta method [42], we observed that inside low-intensity pulses the electron oscillates at a frequency close to the natural (central) frequency of the electric field. As a result of this fast oscillation, only a very small quantity of energy is transferred to the electron and no net acceleration is produced [see Figs. 4(a) and 4(b)]. However, for extremely high laser intensities (say  $10^{22} \text{W}/\text{cm}^2$ ), highly relativistic velocities can be reached within a distance comparable to the laser wavelength. Then, the electron remains confined within a half cycle of the field for a finite period of time. As a result of this partial phase matching (that lasts only a few picosec-

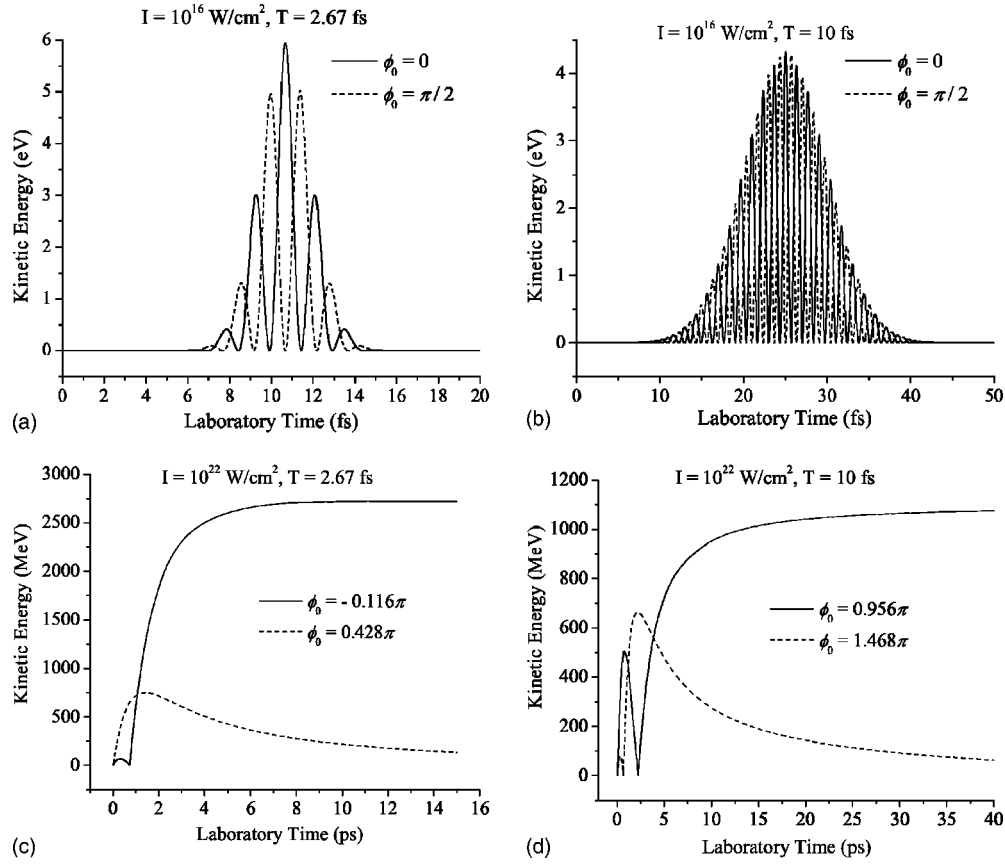


FIG. 4. Energy transferred to an electron at rest at the waist of an ultrashort  $\text{TM}_{01}$  wave packet as a function of time, measured in the laboratory reference frame. (a) and (b) The pulse intensity is too weak to trap and accelerate the electron. (c) and (d) The pulse intensity is above threshold; the electron is trapped and accelerated. Two values of the pulse carrier phase  $\phi_0$ , corresponding to the maximum and the minimum of the transferred energy, are considered for each intensity.

onds), the electron is pushed beyond the Rayleigh distance  $z_R$ . Far from focus ( $z' \gg z_R$ ), the pulse intensity vanishes due to diffraction and the electron moves freely through space with a velocity close to the speed of light (an energy of 1 GeV corresponds to  $v_z/c \approx 0.999\,999\,87$ ), when the pulse has the proper carrier phase at the beam waist [see Figs. 4(c) and 4(d)]. This acceleration mechanism is consistent with the observation that the longitudinal electric field of a  $\text{TM}_{01}$  laser beam decreases as  $(z_R/z')^2$  and experiences a Gouy phase shift of  $\pi$  from the beam waist to infinity.

The net energy gained by the electrons resulting from their acceleration is sensitive to the field intensity, the pulse duration, and the carrier phase (see Fig. 5). Such dependencies are a characteristic of strong-field phenomena [25,32]. A close look at Figs. 4(c) and 4(d) reveals details about the electron dynamics (the horizontal scale on those figures is time). Electrons at rest at the waist that are promptly accelerated to highly relativistic energies tend to progressively get out of phase with the field; they are decelerated in the last part of their trajectory and experience a small overall energy gain. On the contrary, electrons that are subject to a smaller acceleration at the waist tend to be slowed down around the Rayleigh distance (it takes 1.3 ps for a relativistic electron to move from  $z=0$  to  $z_R$ ). From then on, they enter a half cycle of the field that produces a strong acceleration; they remain trapped in the field up to infinity, resulting in a substantial

energy gain. It is observed from Fig. 5 that the use of longer pulses leads to lower values of the peak energy gain, but that the energy gain is less sensitive to the value of the carrier phase. With longer pulses, electrons are trapped in the front of the pulse before the field reaches its peak value. With shorter pulses, some electrons can penetrate the field up to its maximum before being trapped and accelerated.

The results of Fig. 5 show how the non-SVEA corrections influence the electron energy gain. As expected, the effects of the corrections are more important as the pulse duration decreases [35]. However, we observe that the global dynamics is mainly governed by the SVEA field, which appears to be a good approximation even in the case of a few-cycle pulse ( $T \geq 2\pi/\omega_0$ ).

### C. Stability of the on-axis trajectory

The stability of the on-axis trajectory is a major concern for the proposed scheme to be of practical interest. If we assume that the transverse velocity  $v_r$  remains small compared to the speed of light ( $v_r/c \ll 1$ ), the transverse motion of the electron close to the axis ( $r \ll \rho_0$ ) is mainly defined by its longitudinal position inside the field, as seen from the following two equations [obtained from Eqs. (22) and (24)]:

$$\frac{dp_r}{dt} \approx q \left[ 1 - \frac{v_z}{c} \right] \frac{k_0 \Delta r}{2} E_z \cot \Psi_0, \quad (29)$$

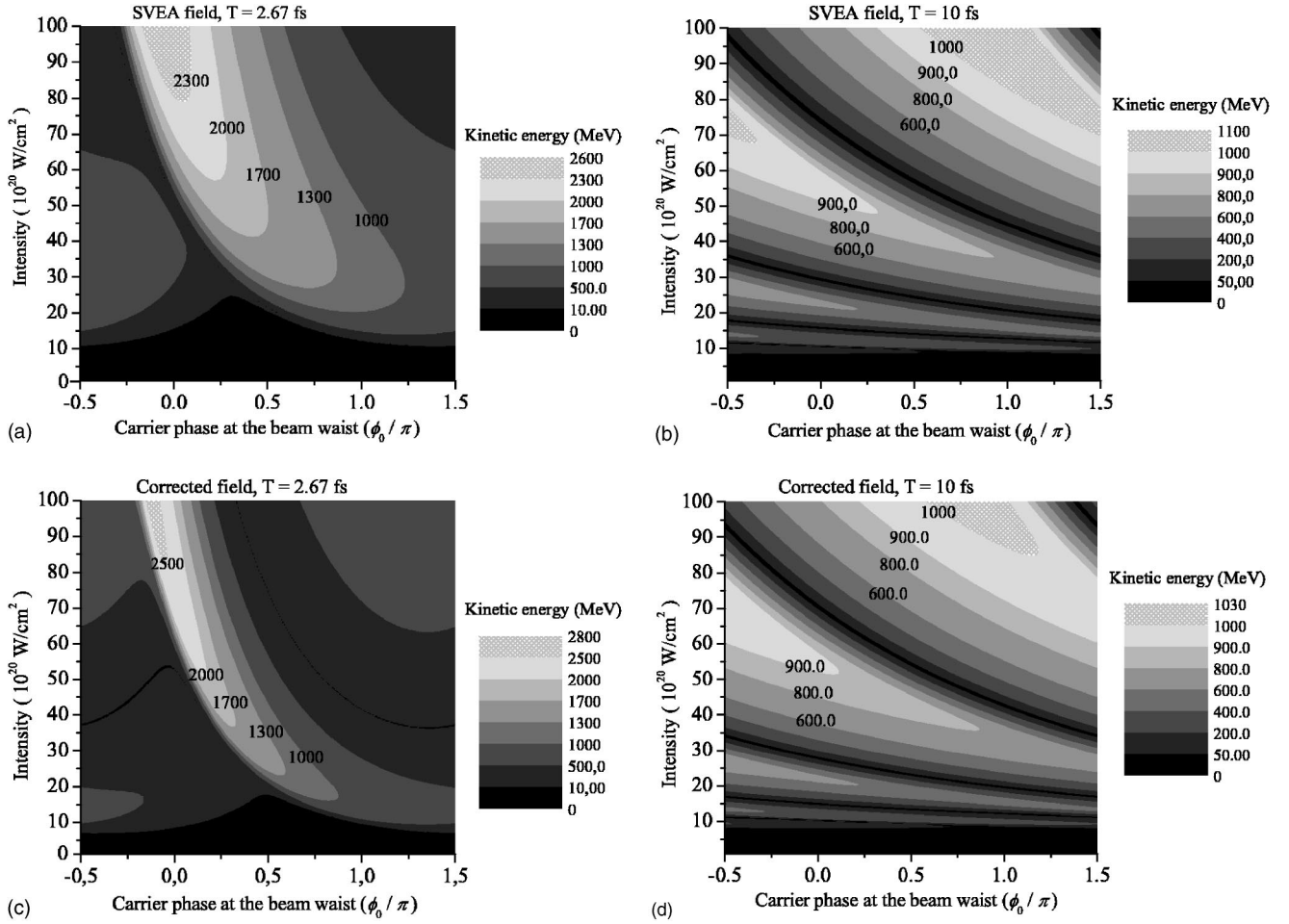


FIG. 5. Energy transferred to an electron at rest at the waist of an ultrashort  $TM_{01}$  wave packet as a function of laser intensity and carrier phase  $\phi_0$ . The energy gain produced by the corrected (non-SVEA) field [in (c) and (d)] is compared to that obtained with the SVEA field [in (a) and (b)].

$$\frac{dp_z}{dt} \approx qE_z, \quad (30)$$

where the SVEA is used for simplicity, with  $\Delta r$  being the small displacement of the electron with respect to the axis. For the definition of  $\Psi_0$ , see below Eq. (28). Because the charge of the electron is negative ( $q < 0$ ), the electron is accelerated when  $E_z < 0$ , i.e., for  $\pi < \Psi_0 < 2\pi$ . From Eq. (29), we then see that off-axis electrons will be focused toward the axis and accelerated for  $3\pi/2 < \Psi_0 < 2\pi$  ( $\cot \Psi_0 < 0$ ). Under relativistic conditions ( $v_z \rightarrow c$ ), the radial acceleration simply vanishes for all values of  $\Psi_0$ . We have observed that the two solid curves shown in Figs. 4(c) and 4(d) (those reporting the highest energy gains) are stable trajectories.

#### D. Radiation

The instantaneous power radiated by an electron accelerated along the axis of a  $TM_{01}$  wave packet is given by the following equation [36]:

$$P_{\text{rad}} = \frac{2}{3} \frac{c}{4\pi\epsilon_0} \left( \frac{q^2}{m_0 c^2} \right)^2 |E_z|^2, \quad (31)$$

where  $\epsilon_0$  is the permittivity of free space ( $\epsilon_0 \approx 10^{-9}/36\pi$  F/m). If we consider only the SVEA field (the main contribution), it then follows that

$$|E_z|^2 \approx 8 \exp(1) \left( \frac{E_0}{k_0 \rho_0} \right)^2 \left( \frac{\rho_0}{\rho(z')} \right)^4 f(t')^2. \quad (32)$$

The result obtained in Eq. (32) shows that the radiation is localized, concentrated in the strong-field regions. The radiation losses thus depend on the relative position of the particle with respect to the focal plane and the center of the wave packet. By assuming that the spatial envelope of the field is constant [ $\rho(z') \approx \rho_0$ ] and that the electron remains at the same position inside the pulse [ $f(t') \approx 1$ ], Eqs. (31) and (32) are simplified to yield

$$P_{\text{rad}} \approx \frac{16 \exp(1)}{3} \frac{c}{4\pi\epsilon_0} \left( \frac{q^2}{m_0 c^2} \right)^2 \left( \frac{E_0}{k_0 \rho_0} \right)^2. \quad (33)$$

On the other hand, we can calculate the power of the driving wave packet. The task is done by integrating the

absolute value of the average Poynting vector  $|\vec{\phi}| = \frac{1}{2} \text{Re}[\mathbf{E} \times \mathbf{H}^*]$  in the plane perpendicular to the propagation axis. From Eqs. (5) and (19), it thus reads

$$P_{\text{field}} = 2\pi \int_0^\infty |\vec{\phi}| r dr, \quad (34a)$$

$$= \frac{\pi \rho_0^2 E_0^2 \exp(1)}{4\eta_0} f(t')^2. \quad (34b)$$

From Eqs. (31) and (34b), we define the following ratio [again,  $\rho(z') \approx \rho_0$  is assumed]:

$$\frac{P_{\text{rad}}}{P_{\text{field}}} \approx \frac{64}{3} \left( \frac{1}{4\pi\epsilon_0} \right)^2 \left( \frac{q^2}{m_0 c^2} \right)^2 \frac{1}{z_R^2}, \quad (35)$$

giving the fraction of the laser light power lost in radiation. For an electron, we calculate that  $P_{\text{rad}}/P_{\text{field}} \sim 10^{-28} z_R^{-2}$ , where  $z_R$  is in meters. For the special case where  $\lambda_0 = 0.8 \mu\text{m}$  and  $\rho_0 = 10 \mu\text{m}$ , the power radiated by an electron is smaller than the power of the driving signal by a factor  $10^{-21}$ . Also, we can evaluate the amount of energy lost because of the radiation. As a global estimate, we set  $\Delta W_{\text{rad}} \sim P_{\text{rad}} \Delta t$ , where  $\Delta t$  is the duration of the interaction. Typically,  $\Delta t \sim 20$  ps [see Figs. 4(c) and 4(d)]. Then, for  $I = 10^{22} \text{W/cm}^2$ ,  $\lambda_0 = 0.8 \mu\text{m}$ , and  $\rho_0 = 10 \mu\text{m}$ , it appears that  $\Delta W_{\text{rad}} \approx 6$  keV. It thus shows that the radiation losses resulting from the acceleration of an electron by the longitudinal electric field of a  $\text{TM}_{01}$  wave packet are negligible. Such low energy losses due to the emission of radiation are typical of linear accelerators [36].

#### IV. DISCUSSION

The propagation of laser light beyond the slowly-varying-envelope approximation is a topic of high interest in many areas of optics, particularly in the study of ultrafast phenomena. To investigate the interaction between ultrashort electromagnetic wave packets and matter, it is necessary to know precisely the distribution of the vectorial electromagnetic field of the laser signal, especially when dealing with free particles [25]. For example, when a very intense optical pulse passes through a film of nanometric thickness, the atoms of the film are ionized. The free electrons produced in this interaction are violently expelled from the focal region. We have shown here that if an ultraintense ultrashort pulse with a  $\text{TM}_{01}$  profile is used, the electrons that are close to the propagation axis are accelerated forward by the longitudinal electric field. In the case of pulses of a few-cycle duration, we have demonstrated that the corrections to the slowly-varying-envelope approximation have an influence on the electron energy gain.

Methods to describe the free-space propagation of vectorial ultrashort pulsed beams in the frequency domain have been proposed by Quesnel and Mora [38] and, more recently, by Lu *et al.* [43]. However, in the time domain it has been demonstrated by Porras [35] that exact expressions that describe the propagation of paraxial ultrashort pulsed beams can be obtained by using a method inspired by the previous

work of Lax *et al.* [33]. In this paper, we have extended that latter work and provided a general expression for the longitudinal electric field of paraxial ultrashort wave packets [see Eq. (10)].

The acceleration of electrons by the longitudinal electric field of a *doughnut-shaped* mode has been previously discussed by Hellwarth and Nouchi [12]. We have noticed that the TM focus wave mode they considered leads to a longitudinal electric field different from that of an ultrashort  $\text{TM}_{01}$  wave packet. Moreover, these authors have suggested the use of a mirror to cut off the accelerating laser beam beyond its waist. From our point of view, the use of a mirror close to the focus of the pulse would encounter severe practical limitations due to material breakdown at such ultrahigh field intensities. According to Varin and Piché [44–47], the presence of a field-limiting apparatus is not required to produce substantial accelerations with TM laser beams. In the light of the results we have presented here, energy can be transferred to an electron initially at rest at the waist of an ultrashort  $\text{TM}_{01}$  wave packet from the longitudinal electric field component. We also observed that there is a clear intensity threshold for this effect to take place. For field intensities that are ten times the threshold (found to be  $10^{21} \text{W/cm}^2$  for  $\lambda = 0.8 \mu\text{m}$  and for a beam with a  $10\text{-}\mu\text{m}$  waist), the energy of the accelerated electrons can exceed 1 GeV.

In the literature, the acceleration of charged particles is often described in terms of the ponderomotive force [37]. This terminology refers to time-averaged equations of motion. Such an approach is particularly useful for a low-mass particle, like an electron, driven by a fast oscillating laser field ( $\omega_0 \sim 10^{15} \text{rad/s}$ ). It should be pointed out that the early theory of the ponderomotive acceleration applies to the non-relativistic regime and is not appropriate to deal with the high intensities provided by today's ultraintense laser technology. In fact, according to Kibble [37] a nonrelativistic regime is characterized by  $\mu = (qE_0/m_0\omega_0c)^2 \ll 1$ , where  $E_0$  is the amplitude of the accelerating field. For an electron driven by the longitudinal field of a TM laser wave packet whose intensity reaches  $10^{22} \text{W/cm}^2$  ( $\lambda_0 = 0.8 \mu\text{m}$ ),  $\mu$  is of the order of 2.5. A few years ago, Quesnel and Mora developed a relativistic treatment of the ponderomotive acceleration dealing with wave packets of finite duration [38]. However, the relativistic theory of the ponderomotive acceleration requires, to be valid, that  $k_0\rho_0(1-v_z/c) \gg 1$ : for an electron accelerated to GeV energies ( $v_z/c \approx 0.99999987$ ) by a paraxial laser wave packet ( $k_0\rho_0 \approx 78.5$ ), it appears that  $k_0\rho_0(1-v_z/c) \approx 10^{-5}$ . On the other hand, the parameter  $\delta = 2\pi\rho_0/cT$ , obtained from the condition  $1/k_0\rho_0 \sim \lambda_0/cT$  introduced by Quesnel and Mora [38], must be of the order of the unity: for a single-cycle wave packet ( $T = 2\pi/\omega_0$ ) whose transverse dimension  $\rho_0$  is  $10 \mu\text{m}$ ,  $\delta$  is about 80. Still, we recall that the final kinetic energy of an electron accelerated by the longitudinal field of an ultrashort  $\text{TM}_{01}$  wave packet is sensitive to the field absolute phase and the pulse temporal extent (see Figs. 4 and 5). As a consequence, the concept of ponderomotive acceleration is not relevant to the acceleration scheme proposed here. We thus conclude that the acceleration mechanism presented in this paper could not have been revealed considering time-averaged equations of mo-



tion (the ponderomotive force) [37], even in the relativistic case [38].

In the past, the acceleration of electrons by ultrashort electromagnetic wave packets has been the object of severe criticisms (see Kim *et al.* [48]). In the case where the time integral of the accelerating electric field does not vanish, an important amount of energy can be transferred to the electron from the static ( $\omega=0$ ) component of the field. It is widely accepted that such acceleration mechanisms are incorrect and lead to nonphysical predictions that cannot be reproduced experimentally. For the signals considered in this paper, we define the following ratio:

$$R = \frac{\left[ \int_{-\infty}^{\infty} f(t') e^{j(\omega_0 - \omega)t'} dt' \right]_{\omega=0}}{\left[ \int_{-\infty}^{\infty} f(t') e^{j(\omega_0 - \omega)t'} dt' \right]_{\omega=\omega_0}} = \exp\left(-\frac{T^2 \omega_0^2}{4}\right), \quad (36)$$

giving the relative amplitude of the zero-frequency component ( $\omega=0$ ) compared to the main component of the spectrum ( $\omega=\omega_0$ ) along the axis ( $r=0$ ) of a  $\text{TM}_{01}$  wave packet. We thus see that for a single-cycle wave packet ( $T=2\pi/\omega_0$ ) the condition of a zero integral of the field is fairly well respected ( $R=5 \times 10^{-5}$ ). For a wave packet with  $T=7.5\pi/\omega_0$  (corresponding to a time duration of 10 fs for  $\lambda_0=0.8 \mu\text{m}$ ), the integral of the electric field simply vanishes ( $R \sim 10^{-60}$ ).

The amount of energy transferred to the electron from the static component of the field  $\Delta W_{\omega=0}$  can be evaluated from the line integral of the driving force  $\Delta W = \int_A^B \mathbf{F} \cdot d\mathbf{l}$  (where  $\mathbf{F}$  is the Lorentz force). In the frequency domain, we can see that

$$\frac{\Delta W(\omega=0)}{\Delta W(\omega=\omega_0)} = R, \quad (37)$$

where  $\Delta W(\omega=0)$  and  $\Delta W(\omega=\omega_0)$  are energies respectively associated with the static and the main component of the spectrum. From Eq. (37), we see that the effect of the static field is negligible. In the time domain, assuming a perfect synchronization between the field (noncorrected) and the electron and neglecting the spatial variations of the absolute phase of the carrier due to the Gouy phase shift, the acceleration produced by the static component is evaluated from the expression that follows:

$$\Delta W_{\omega=0} \approx 2|q| \frac{A}{k_0} R \int_0^{\infty} \frac{dz'}{1 + z'^2/z_R^2}, \quad (38a)$$

$$\approx |q| \frac{\pi \exp(1/2)}{\sqrt{2}} \rho_0 E_0 R, \quad (38b)$$

where  $E_0$  is the amplitude of the transverse field in V/m. We then see that the static component of the single-cycle wave

packet ( $\rho_0=10 \mu\text{m}$ ,  $I=10^{22} \text{ W/cm}^2$ ,  $T=2.67 \text{ fs}$ , and  $\Delta W_{\omega=0} \approx 520 \text{ keV}$ ), contributes only as a small fraction (less than 0.02%) of the total amount of energy transferred to the electron [see Fig. 4(c)]. For a pulse with  $T=10 \text{ fs}$  and  $\lambda_0=0.8 \mu\text{m}$ , as seen in Fig. 4(d), the effect of the static component is vanishingly small ( $\Delta W_{\omega=0} \sim 10^{-50} \text{ eV}$ ). Hence, as expected from Eq. (37) the contribution of the static component is not significant. In fact, Eq. (38b) gives a generous estimate of what could be the real effect of the static field. From our numerical simulations, it appears that the synchronization of the electron with the field is only maintained within a region that goes approximately from  $z \approx z_R$  to  $z = \infty$  [see Figs. 4(c) and 4(d)]. As a result of this shortened interaction,  $W_{\omega=0}$  would be half (260 keV) of what is obtained when a perfect phase matching is assumed (520 keV). Moreover, the effect of the Gouy phase shift has been neglected: the slow evolution of the carrier wave absolute phase (due to diffraction) would probably reduce considerably the contribution of the static field. This clearly shows that even if the integral of the longitudinal field is not rigorously zero, the corresponding static field is not responsible for the important accelerations reported in this paper.

## V. CONCLUSION

The on-axis acceleration of an electron by the longitudinal electric field of a single-cycle  $\text{TM}_{01}$  laser wave packet in free space has been studied. Direct-time integration of the instantaneous Lorentz force revealed an intensity-induced phase matching between the electron and the field, when the pulse intensity exceeds  $10^{21} \text{ W/cm}^2$ . The kinetic energy transferred to the accelerated electron depends on the absolute phase of the pulse carrier. For ultrahigh intensities (say  $10^{22} \text{ W/cm}^2$ ), an electron could be accelerated from rest to GeV energies within a few millimeters. The acceleration scheme could be implemented as a probe-driver experiment, where a first laser pulse would be used to prepare a bunch of thermal—close to rest—electrons which are subsequently accelerated by a high-intensity ultrashort  $\text{TM}_{01}$  laser wave packet. Alternatively, free electrons could probably be produced and accelerated by a unique laser pulse, illuminating a very thin foil.

## ACKNOWLEDGMENTS

M.P. and C.V. thank Les Fonds de Recherche sur la Nature et les Technologies (Québec), the Natural Sciences and Engineering Research Council (Canada), and the Canadian Institute for Photonic Innovations for their financial support.

- [1] A. M. Sessler, *Phys. Today* **41** (1), 26 (1988).
- [2] J. S. Wurtele, *Phys. Today* **47** (7), 33 (1994).
- [3] M. Tigner, *Phys. Today* **54** (1), 36 (2001).
- [4] W. K. H. Panofsky and M. Breidenbach, *Rev. Mod. Phys.* **71**, S121 (1999).
- [5] K. Shimoda, *Appl. Opt.* **1**, 33 (1962).
- [6] L. C. Steinhauer and W. D. Kimura, *Phys. Rev. ST Accel. Beams* **6**, 061302 (2003).
- [7] T. Tajima and J. M. Dawson, *Phys. Rev. Lett.* **43**, 267 (1979).
- [8] C. Joshi and T. Katsouleas, *Phys. Today* **56** (6), 47 (2003).
- [9] E. D. Courant, C. Pellegrini, and W. Zakowicz, *Phys. Rev. A* **32**, 2813 (1985).
- [10] A. Loeb and L. Friedland, *Phys. Rev. A* **33**, 1828 (1986).
- [11] P. Sprangle, E. Esarey, and J. Krall, *Phys. Plasmas* **3**, 2183 (1996).
- [12] R. W. Hellwarth and P. Nouchi, *Phys. Rev. E* **54**, 889 (1996).
- [13] H. M. Lai, *Phys. Fluids* **23**, 2373 (1980).
- [14] B. Rau, T. Tajima, and H. Hojo, *Phys. Rev. Lett.* **78**, 3310 (1997).
- [15] Y. Cheng and Z. Xu, *Appl. Phys. Lett.* **74**, 2116 (1999).
- [16] J. Wang, W. Scheid, M. Hoelss, and Y. Ho, *Phys. Lett. A* **275**, 323328 (2000).
- [17] J. Zawadzka, D. A. Jaroszynski, J. J. Carey, and K. Wynne, *Appl. Phys. Lett.* **79**, 2130 (2001).
- [18] X. E. Lin, *Phys. Rev. ST Accel. Beams* **4**, 051301 (2001).
- [19] M. J. Feldman and R. Y. Chiao, *Phys. Rev. A* **4**, 352 (1971).
- [20] M. O. Scully and M. S. Zubairy, *Phys. Rev. A* **44**, 2656 (1991).
- [21] C. M. Haaland, *Opt. Commun.* **114**, 280 (1995).
- [22] J. X. Wang, Y. K. Ho, Q. Kong, L. J. Zhu, L. Feng, S. Scheid, and H. Hora, *Phys. Rev. E* **58**, 6575 (1998).
- [23] S. Takeuchi and R. Sugihara, *Phys. Rev. E* **58**, 7874 (1998).
- [24] B. Hafizi, A. K. Ganguly, A. Ting, C. I. Moore, and P. Sprangle, *Phys. Rev. E* **60**, 4779 (1999).
- [25] H. Hora, M. Hoelss, W. Scheid, J. Wang, Y. Ho, F. Osman, and R. Castillo, *Laser Part. Beams* **18**, 135 (2000).
- [26] S. Tidwell, D. Ford, and D. Kimura, *Appl. Opt.* **29**, 2234 (1990).
- [27] A. Siegman, *Lasers* (University Science, Mill Valley, CA, 1986).
- [28] W. L. Erikson and S. Singh, *Phys. Rev. E* **49**, 5778 (1994).
- [29] L. W. Davis, *Phys. Rev. A* **30**, 3092 (1984).
- [30] E. J. Bochove, G. T. Moore, and M. O. Scully, *Phys. Rev. A* **46**, 6640 (1992).
- [31] T. Brabec and F. Krausz, *Phys. Rev. Lett.* **78**, 3282 (1997).
- [32] T. Brabec and F. Krausz, *Rev. Mod. Phys.* **72**, 545 (2000).
- [33] M. Lax, W. H. Louisell, and W. B. McKnight, *Phys. Rev. A* **11**, 1365 (1975).
- [34] E. Haselhoff, *Phys. Rev. E* **49**, R47 (1994).
- [35] M. A. Porras, *Opt. Lett.* **26**, 44 (2001).
- [36] J. Jackson, *Classical Electrodynamics*, 3rd ed. (Wiley, New York, 1999).
- [37] T. W. B. Kibble, *Phys. Rev.* **150**, 1060 (1966).
- [38] B. Quesnel and P. Mora, *Phys. Rev. E* **58**, 3719 (1998).
- [39] F. Lindner, G. G. Paulus, H. Walther, A. Baltuška, E. Goulielmakis, M. Lezius, and F. Krausz, *Phys. Rev. Lett.* **92**, 113001 (2004).
- [40] N. Cao, Y. Ho, Q. Kong, P. Wang, X. Yuan, Y. Nishida, N. Yugami, and H. Ito, *Opt. Commun.* **204**, 715 (2002).
- [41] J. X. Wang, W. Scheid, M. Hoelss, and Y. K. Ho, *Phys. Rev. E* **64**, 066612 (2001).
- [42] W. H. Press, S. A. Teukolsky, W. T. Vetterling, and B. P. Flannery, *Numerical Recipes in C, The Art of Scientific Computing*, 2nd ed. (Cambridge University Press, Cambridge, U.K., 1992).
- [43] D. Lu, W. Hu, Z. Yang, and Y. Zheng, *J. Opt. A, Pure Appl. Opt.* **5**, 263 (2003).
- [44] C. Varin and M. Piché, *Appl. Phys. B: Lasers Opt.* **74** (Suppl.), S83 (2002).
- [45] C. Varin and M. Piché, *Proc. SPIE* **4833**, 476 (2002).
- [46] C. Varin and M. Piché, *Ultrafast Phenomena XIII*, Series in Chemical Physics, Vol. 74 (Springer, Berlin, 2003), pp. 164–166.
- [47] C. Varin and M. Piché, in *Proceedings of the 35th ISQE* (World Scientific, Singapore, 2004), pp. 249–254.
- [48] K.-J. Kim, K. T. McDonald, and G. V. Stupakov, *Phys. Rev. Lett.* **84**, 3210 (2000).